Published in final edited form as:
J Proteome Res. 2012 December 7; 11(12): 5994–6007. doi:10.1021/pr300702c.

MASS SPECTROMETRY-BASED IDENTIFICATION OF NATIVE CARDIAC Nav1.5 CHANNEL α SUBUNIT PHOSPHORYLATION SITES

Céline Marionneau[1,2,3,†], **Cheryl F Lichti**[4,*], **Pierre Lindenbaum**[1,2,3], **Flavien Charpentier**[1,2,3], **Jeanne M Nerbonne**[6], **R Reid Townsend**[4,5], and **Jean Mérot**[1,2,3]

[1]INSERM, UMR1087, L'Institut du Thorax, Nantes, France

[2]CNRS, UMR6291, Nantes, France

[3]LUNAM Université, Nantes, France

[4]Department of Internal Medicine, Washington University Medical School, Saint Louis, MO, USA

[5]Department of Cell Biology, Washington University Medical School, Saint Louis, MO, USA

[6]Department of Developmental Biology, Washington University Medical School, Saint Louis, MO, USA

Abstract

Cardiac voltage-gated Na^+ (Nav) channels are key determinants of action potential waveforms, refractoriness and propagation, and Nav1.5 is the main Nav pore-forming (α) subunit in the mammalian heart. Although direct phosphorylation of the Nav1.5 protein has been suggested to modulate various aspects of Nav channel physiology and pathophysiology, native Nav1.5 phosphorylation sites have not been identified. In the experiments here, a mass spectrometry (MS)-based proteomic approach was developed to identify native Nav1.5 phosphorylation sites directly. Using an anti-NavPAN antibody, Nav channel complexes were immunoprecipitated from adult mouse cardiac ventricles. The MS analyses revealed that this antibody immunoprecipitates several Nav α subunits in addition to Nav1.5, as well as several previously identified Nav channel associated/regulatory proteins. Label-free comparative and data-driven phosphoproteomic analyses of purified cardiac Nav1.5 protein identified 11 phosphorylation sites, 8 of which are novel. All the phosphorylation sites identified except one in the N-terminus are in the first intracellular linker loop, suggesting critical roles for this region in phosphorylation-dependent cardiac Nav channel regulation. Interestingly, commonly used prediction algorithms did not reliably predict these newly identified *in situ* phosphorylation sites. Taken together, the results presented provide the first *in situ* map of basal phosphorylation sites on the mouse cardiac Nav1.5 α subunit.

Keywords

Nav1.5 Channels; Heart; Native Phosphorylations; Mass Spectrometric Identifications; Label-free Comparative and Data-driven LC-MS/MS Analyses

[†]**Correspondence to:** Céline Marionneau, INSERM UMR1087, L'Institut du Thorax, CNRS UMR6291, Institut de Recherches Thérapeutiques, 8 Quai Moncousu, BP 70721, 44007 Nantes Cedex 1, Tel: +33 2 28 08 01 63, Fax : +33 2 28 08 01 30, celine.marionneau@univ-nantes.fr.
[*]**Present Address:** Department of Pharmacology and Toxicology, University of Texas Medical Branch, Galveston, TX 77555-0372

Conflict of Interest Disclosure
The authors declare no competing financial interest.

Introduction

Voltage-gated Na^+ (Nav) channels are critical determinants of membrane excitability in the mammalian myocardium in that these channels underlie action potential generation, refractoriness and propagation[1]. Defects in Nav channel expression or functioning, associated with inherited or acquired cardiac disease, are linked to increased risk of life threatening arrhythmias[2]. Although nine functionally related Nav pore-forming (α) subunit genes have been identified, *SCN5A*, which encodes Nav1.5, is the primary determinant of mammalian cardiac Nav channels. Like the other Nav α subunits, the Nav1.5 protein has four homologous domains (DI to DIV), each of which contains six transmembrane-spanning segments, three intracellular linker loops (between the domains) and cytoplasmic N- and C-termini. Accumulated evidence suggests that native cardiac Nav1.5 channels function in macromolecular protein complexes comprising a variety of interacting and regulatory proteins[3, 4].

Post-translational modifications, such as ubiquitylation or phosphorylation, of Nav1.5 have also been suggested to be important in the regulation of cardiac Nav channel expression and biophysical properties[3, 4]. Activation of Protein Kinase A (following β-adrenergic stimulation), for example, increases Nav current densities in ventricular myocytes, an observation interpreted as consistent with direct phosphorylation of the channels and enhanced trafficking to the cell surface[5–8]. Several recent reports have also linked Ca^{2+}/Calmodulin-dependent protein Kinase II (CamKII) to the regulation of cardiac Nav channel gating, which is altered dramatically in the failing heart[9, 10]. Biochemical studies have also revealed CamKII-mediated phosphorylation of Nav1.5 and suggested roles for serine-516, serine-571 and threonine-594 as critical sites for CamKII-mediated modulation of the kinetics and voltage-dependence of cardiac Nav channel inactivation[11, 12]. Although these combined observations suggest critical roles for kinase-mediated phosphorylation in regulating the expression and the properties of myocardial Nav channels, the basal, *in situ* phosphorylation sites on the cardiac Nav1.5 protein have not been identified.

Increasingly, the application of MS-based proteomic analyses has revealed that the numbers and complexities of phosphorylation sites on membrane proteins, including ion channels, are much greater than expected and, in addition, are distinct from patterns predicted based upon consensus sequences[13–15]. A number of recent studies on the voltage-gated K^+ channel subunits Kv2.1[16] and Kv1.2[17], as well as on the pore-forming subunit (BK_{Ca}) of the large-conductance Ca^{2+}-activated K^+ channel[18], have revealed the power of such proteomic approaches for the identification of native phosphorylation sites. Although enrichment methods, based on chromatography, have improved and advanced phosphoproteomic analyses, these approaches still lack sensitivity and specificity[19]. Recent innovative advancements associated with label-free quantitative MS analyses[20–23] combined with the increased capabilities to acquire high mass resolution and directed mass spectral data[24–28] are now making it possible to achieve sensitive phosphoproteomic analyses of simple protein mixtures without using enrichment methods.

In the experiments here, a MS-based proteomic approach was developed and utilized to identify directly the basal *in situ* phosphorylation sites on the cardiac Nav1.5 α subunit purified from adult mouse cardiac ventricles using a pan-anti-Nav α subunit antibody. In addition to identifying Nav1.5, other Nav α subunits and Nav associated/regulatory proteins by liquid chromatography tandem MS analyses, the development of a non-conventional experimental approach, exploiting label-free quantification of high-resolution MS data, followed by data-driven analyses of a comprehensive set of phosphorylated Nav1.5 peptides,

led to the identification of multiple *in situ* phosphorylation sites on the native mouse ventricular Nav1.5 protein.

Materials and Methods

Animals were handled in accordance with the guidelines published in the European Community Guide for the Care and Use of Laboratory Animals. Experimental protocols were approved by the local animal care and use committee (Comité d'Ethique pour l'Expérimentation Animale des Pays de la Loire).

Immunoprecipitation of Cardiac Nav Channel Complexes

Flash-frozen ventricles from adult wild-type mice were homogenized in ice-cold lysis buffer containing 20 mM HEPES (pH 7.4), 150 mM NaCl, 0.5% amidosulfobetaine (Sigma), 1X complete protease inhibitor cocktail tablet (Roche), 1 mM PMSF (Interchim), 0.7 μg/ml pepstatin A (Thermo Scientific) and 1X Halt phosphatase inhibitor cocktail (Thermo Scientific). After 15-min rotation at 4°C, 8 mg of the soluble protein fraction were pre-cleared with 200 μL of protein G-magnetic beads (Invitrogen) for 1 hr and subsequently used for immunoprecipitations (IP) with 48 μg of an anti-NavPAN monoclonal antibody (mαNavPAN, Sigma), raised against the SP19 epitope[29] located in the third intracellular linker loop and common to all Nav α subunits. Parallel control experiments were completed using 48 μg of a non-specific mouse immunoglobulin G (mIgG, Santa Cruz Biotechnology). Prior to the IP, antibodies were cross-linked to 200 μl of protein G-magnetic beads using 20 mM dimethyl pimelimidate (Thermo Scientific)[30]. Protein samples and antibody-coupled beads were mixed for 2 hr at 4°C. Magnetic beads were then collected, washed rapidly four times with ice-cold lysis buffer, and isolated protein complexes were eluted from the beads in 1X Sodium Dodecyl Sulfate (SDS) buffer at 60°C for 5 min (for gel electrophoresis analyses), or in 2% Rapigest[31] (Waters), 8 M urea (Sigma), 100 mM Tris (pH 8.5) at 37°C for 30 min (for mass spectrometric analyses).

Gel Electrophoreses and Western Blot Analyses

Eluted proteins were separated on one-dimensional polyacrylamide gels after treatment with 100 mM dithiothreitol (DTT) at 60°C for 5 min and analyzed by either Coomassie blue (Fermentas) staining or Western blotting using a rabbit polyclonal anti-Nav1.5 antibody (RbαNav1.5, Alomone, #ASC-005). Bound antibodies were detected using horseradish peroxidase-conjugated goat anti-rabbit secondary antibody (Santa Cruz Biotechnology), and protein signals were visualized using the ECL Plus Western blotting detection system (GE Healthcare).

In-Solution Endoprotease Digestion

Eluted proteins (in 2% Rapigest, 8 M urea, 100 mM Tris, pH 8.5) were precipitated using the 2D protein clean up kit (GE Healthcare). The resulting pellets were dissolved in 8 M urea, 100 mM Tris (pH 8.5), reduced with 5 mM tris (2-carboxyethyl) phosphine (pH 8.0) for 30 min at room temperature, and alkylated with 10 mM iodoacetamide (BioRad) for 30 min at room temperature. Samples were then digested with 1 μg endoproteinase Lys-C (Roche) overnight at 37°C, and subsequently with 4 μg of trypsin (Sigma) overnight at 37°C. Peptides were acidified with formic acid, extracted with NuTip porous graphite carbon wedge tips (Glygen), and eluted with aqueous acetonitrile (ACN, 60%) containing formic acid (FA, 0.1%). The extracted peptides were dried, dissolved in aqueous ACN/FA (1%/1%), stored at −80°C and subsequently analyzed using one-dimensional LC-MS/MS.

LC-MS/MS Analyses

Peptide mixtures were analyzed using high-resolution nano-LC-MS on a hybrid mass spectrometer consisting of a linear quadrupole ion trap and an Orbitrap (LTQ-Orbitrap XL, Thermo Fisher Scientific). Chromatographic separations were performed using a nanoLC 1D Plus™ (Eksigent) for gradient delivery and a cHiPLC-nanoflex (Eksigent) equipped with a 15 cm × 75 μm C18 column (ChromXP C18-CL, 3 μm, 120 Å, Eksigent). The liquid chromatograph was interfaced to the mass spectrometer with a nanospray source (PicoView PV550; New Objective). Mobile phases were 1% FA in water (A) and 1% FA in ACN (B). After equilibrating the column in 100% solvent A (aqueous 1% FA) and 0% of solvent B (ACN containing 1% FA), the samples (5 μL) were injected from autosampler vials using the LC-system-autosampler at a flow rate of 750 nL/min for 20 min followed by gradient elution (250 nL/min) with solvent B: isocratic at 2% B, 0–5 min; 2% to 25% B, 5–110 min; 25% to 80% B, 110–170 min; 80% to 2% B, 170–175 min; and isocratic at 2% B, 175–190 min. Total run time, including column equilibration, sample loading, and analysis was 217 min.

The survey scans (m/z 350–2000) (MS1) were acquired at high-resolution (60,000 at m/z 400) in the Orbitrap, and the MS/MS (MS2) spectra were acquired in the linear ion trap at low-resolution, both in profile mode. The maximum injection times for the MS1 scans in the Orbitrap and the LTQ were 500 and 200 ms, respectively. The automatic gain control targets for the Orbitrap and the LTQ were 5×10^5 and 3×10^4, respectively. The MS1 scans were followed by six MS2 events in the linear ion trap with collision activation in the ion trap (parent threshold 1000, isolation width 2.0 Da, normalized collision energy 30%, activation Q 0.250, and activation time 30 ms). Maximum injection times for the MS2 scans were 100 msec, and the automatic gain control target for the LTQ was 1×10^4. Dynamic exclusion was used to remove selected precursor ions (−0.20/+1.0 Da) for 90 s after MS2 acquisitions. A repeat count of 1, a repeat duration of 45 s, and a maximal exclusion list size of 500 were used. The following ion source parameters were used: capillary temperature 200°C, source voltage 3.0 kV, source current 100 μA, capillary voltage 33 V, and tube lens 120 V. Data were acquired using XCalibur, version 2.0.7 (Thermo Fisher).

For high-resolution data-driven analyses, survey scans (m/z 350–2000) (MS1) were acquired at high-resolution (60,000 at m/z = 400) in the Orbitrap in profile mode and MS2 spectra were acquired at 7500 resolution in the Orbitrap in profile mode after fragmentation in the linear ion trap. The maximum injection times for the MS1 scans in the Orbitrap and the LTQ were both 500 ms, and the maximum injection times for the MSn scans in the Orbitrap and the LTQ were 500 ms and 1000 ms, respectively. The automatic gain control targets for the Orbitrap and the LTQ were 2×10^5 and 3×10^4, respectively, for the MS1 scans and 1×10^5 and 1×10^4, respectively, for the MSn scans. The MS1 scans were followed by three MS2 events in the linear ion trap with collision activation in the ion trap (parent threshold 10000, isolation width 4.0 Da, normalized collision energy 30%, activation Q 0.250, activation time 30 ms). Targeted masses were placed in a global mass list with retention time windows specified, and MS2 spectral acquisitions were triggered if the parent mass was within 20 ppm. Dynamic exclusion was disabled. The following ion source parameters were used: capillary temperature 200°C, source voltage 4.5 kV, source current 100 μA, and tube lens 165 V. Data were acquired using XCalibur, version 2.0.7 (Thermo Fisher).

Data Analyses for Protein Identification

The LC-MS raw files were processed using MASCOT Distiller (version 2.3.0.0, Matrix Science) with settings previously described[23]. The resulting MS2 centroided files were used for database searching with MASCOT (version 2.1.6) against either the Uniprot-Mouse database or a custom, in-house database containing Nav1.5 using the following parameters:

trypsin as the enzyme, MS tolerance of 20 ppm, MS/MS tolerance of 0.8 Da (low-resolution MS/MS) or 100 mmu (high-resolution MS/MS), with a fixed carbamidomethylation of Cys residues and variable modifications being oxidation (Met) and phosphorylation (Ser, Thr and/or Tyr), a maximal number of missed cleavages of 9, and +1, +2, and +3 charge states. Scaffold (version 3.4.5, Proteome Software) was used to validate MS/MS-based peptide and protein identifications. Peptide identifications were accepted when established at greater than 95% probability using the Peptide Prophet algorithm[32]. Protein identifications were accepted when established at greater than 95% probability and contained at least one identified peptide. Protein probabilities were assigned by the Protein Prophet algorithm[33]. Proteins that contained similar peptides and could not be differentiated based on MS/MS analysis alone were grouped to satisfy the principles of parsimony.

Identification of Putative Phosphopeptides for Data-Driven Analyses

Candidate phosphopeptides to be characterized by data-driven analyses were selected in Rosetta Elucidator™ (version 3.3, Rosetta Biosoftware) by querying observed *m/z* values with a theoretical list obtained from *in silico* digestion of mouse Nav1.5. To perform label-free quantitative analyses of mass spectra of precursor ions (MS1) data, the LC-MS/MS data from triplicate analyses of control (mIgG-IPs) and of experimental (mαNavPAN-IPs) immunoprecipitates were imported into Rosetta Elucidator for retention time and *m/z* alignment of the peptide ion chromatograms as previously described[22]. Normalization of signal intensities across samples was performed using the average signal intensities obtained in each sample. The *in silico* digestion was performed using mMass[34] with trypsin as the proteolytic enzyme, a maximal number of 5 missed cleavages, carbamidomethylation of Cys residues as a fixed modification, oxidation of Met residues as well as single or double phosphorylation (on Ser, Thr and/or Tyr) as variable modifications, and +2 and +3 charge states. Theoretical *m/z* values were sorted by charge state for mass-matching within Rosetta Elucidator with a tolerance of 20 ppm. After matching, results were filtered to ensure that all matches were correct by mass and charge and that all matched phosphopeptides were not part of predicted Nav1.5 transmembrane domains. Results were subsequently filtered to keep only those *m/z* values of peptides that were present in the 3 mαNavPAN-IPs and absent in the 3 mIgG-IPs. Ion chromatograms and isotopic distributions of the remaining peptides were then visually inspected to remove misaligned or noisy data. As a final check, the presence/absence of the +2 and/or +3 unphosphorylated peptide versions of each matched phosphopeptide was examined manually in XCalibur: only those *m/z* values for which at least one of the unphosphorylated counterparts was found within 5 min of the putative phosphopeptide were retained as candidates for accurate inclusion mass screening MS2 analyses from original pooled mαNavPAN-IP samples.

Phosphopeptide Spectral Interpretation and Site Localization

Phosphopeptide spectra from data-dependent and accurate inclusion mass screening were manually interpreted by comparing the observed mass values from the spectrum in XCalibur with the theoretical parent and fragment Nav1.5 ion mass values from MS-Product (prospector.ucsf.edu). In those instances of data-dependent low-resolution MS2 spectrum analyses where duplicate peptides were detected, the peptide with the highest Scaffold probability and Mascot ion scores was selected for analysis. When a phosphopeptide ion was triggered multiple times in series for accurate inclusion mass screening, similar spectra were summed across the most intense portion of the chromatographic peak, and the resulting summed spectrum was used for ion and phosphorylation site assignments. Annotations of MS2 spectra were first automated using a java-based software (http://code.google.com/p/code915/source/browse/trunk/proteomics/src/fr/inserm/umr915/proteomics/MassSpecProduct.java) which matches observed *m/z* values with theoretical fragment masses from MS-Product, and definitive annotations were subsequently obtained by manual

verification and interpretation. Mass accuracy tolerances of 20 ppm or 0.5 Da were used as guidelines for high- and low-resolution spectral annotations, respectively, and only those ions with mass errors within these ranges were included to determine residue coverage and location(s) of phosphorylation site(s). Additionally, for spectral annotation of high-resolution MS2 data, charge states of observed parent and fragment ions were determined, and only precursor, b- and y-ions with confirmed charge states (i.e. with at least the presence of the ^{13}C isotope peak) were used. The presence of a very intense peak signal (if not the base peak) corresponding to the neutral loss of phosphoric acid from the intact parent ion (loss of 98 for +1 ions, 49 for +2 ions, and 32.66 for +3 ions) during collision induced dissociation was considered as a strong indication of phosphorylation. The phosphorylation site assignments were based on the presence or absence of the unphosphorylated and phosphorylated b- and y-ions flanking the site(s) of phosphorylation, ions that we call site-discriminating ions throughout this manuscript. When site-discriminating ions were not all detected, assignments of phosphorylation sites were narrowed down to one, two (for pS524 and/or pS525) or four (for pS36, pT38, pS39 and/or pS42) possibility(ies) by elimination. In addition to mass accuracy and charge state, the relative percentage of maximum intensity of site-discriminating ions or of any supporting ions in each analyzed spectrum was also considered for spectral annotation. The representative MS1 and MS2 spectra used for each of the phosphorylation site assignments are presented in Figure 3 and Supplemental Figures. The definition of all observed site-discriminating ions, as well as the calculated mass errors, charge state confirmations and/or percentages of maximum intensities for all supporting b- and y-ions (as well as for the loss of phosphoric acid peaks) are summarized in Table 2 and Supplemental Tables.

Results

Purification and Characterization of Cardiac Nav Channel Complexes

Native Nav channel complexes were immunoprecipitated (IP) from adult wild-type mouse cardiac ventricles using a monoclonal anti-NavPAN specific antibody (mαNavPAN) directed against the third intracellular linker loop of Nav α subunits, and the protein components of the isolated channel complexes were identified using a MS-based proteomic approach[35]. A non-specific mouse immunoglobulin G (mIgG) was used in control IPs from the same cardiac protein lysates. As illustrated in Figure 1B, Western blot analyses of the immunoprecipitated proteins probed with a polyclonal anti-Nav1.5 specific antibody (RbαNav1.5) reliably revealed robust Nav1.5 IP from mouse cardiac ventricles with mαNavPAN. The IP of Nav1.5 was specific as evidenced by the absence of signal in the mIgG-IP. Importantly, Western blot analyses of the IP supernatants revealed > 80% depletion of the Nav1.5 protein (lower panel of Figure 1B), suggesting that the isolated Nav1.5 channel complexes likely are representative of the entire mouse ventricle population of Nav1.5 channels. Analyses of immunoprecipitated proteins on Coomassie blue-stained gels revealed the presence of a band corresponding to the molecular weight of Nav α subunits and specific to the mαNavPAN-IPs, i.e., the band was absent in the control IPs (Figure 1A). Mass spectrometric analyses of this Coomassie blue-stained protein band led to the reliable identification of multiple peptides derived from the Nav1.5 protein (data not shown). In contrast, analyses of the corresponding gel area from the control mIgG-IPs did not reveal any peptides corresponding to the Nav1.5 protein or to other Nav α subunits. Taken together, these observations demonstrate that mαNavPAN-IPs from wild-type mouse ventricles were enriched in the protein components of Nav channel complexes.

To identify the protein components of native Nav channel complexes, the entire immunoprecipitated protein samples (i.e., without gel fractionation) were analyzed using one-dimensional LC-MS/MS. Interestingly, in addition to the Nav1.5 protein which was the most abundant protein in the mαNavPAN-IPs, these analyses also resulted in the

identification of three other Nav α subunits, Nav1.4, Nav1.3 and Nav1.7 (Table 1). Compared with Nav1.5, however, only a few peptides of these Nav α subunits were detected, suggesting lower relative abundances in mouse ventricles (Table 1). These experiments also led to the reliable identification of some previously identified Nav channel associated/regulatory proteins[3, 4], including calmodulin, the δ, β and γ subunits of the Ca^{2+}/Calmodulin-dependent protein Kinase II (CamKIIδ, CamKIIβ and CamKIIγ) and Fibroblast Growth Factor 13 (FGF13)[36] (Table 1). The numbers of unique and total peptides detected using these analyses as well as the amino acid sequence coverage obtained for each protein are shown in Table 1; none of these peptides were detected in the control mIgG-IPs. As an example, 86 (and 298 total) Nav1.5 peptides were detected, corresponding to 25% amino acid sequence coverage of the Nav1.5 protein (Table 1). Although the sequence coverage of the Nav1.5 protein is quite good, nearly all of the peptides identified are located in the C- and N-termini or in the first intracellular linker loop of the protein (Figure 1C). No peptides in the transmembrane domains of Nav1.5 were identified, which, as previously suggested for other channels[35], likely reflects the hydrophobic nature of the transmembrane domains.

A Label-Free Comparative and Data-Driven Phosphoproteomic Strategy for the Analysis of Purified Cardiac Nav1.5 Protein

In an effort to obtain a comprehensive phosphorylation map of the cardiac Nav1.5 α subunit, a label-free comparative and data-driven MS-based phosphoproteomic strategy was developed (Figure 2). In this strategy, MS1 data obtained from high-resolution mass spectra of precursor ions from triplicate analyses of mαNavPAN-IPs and mIgG-IPs were extracted, aligned based upon *m/z* and retention times, and label-free quantified using Rosetta Elucidator computational methods[22]. These off-line analyses provided a list of detected MS1 peptide features defined by a *m/z* value, a charge state, a retention time, intensities (in the six samples analyzed), and when annotated by tandem mass spectrometry (MS2) analyses, a peptide sequence and protein name. As an illustration of this point, a MS2 annotated Nav1.5 peptide was detected in the triplicate mαNavPAN-IPs and absent in the mIgG-IPs, whereas an albumin peptide was equally represented in the mαNavPAN- and mIgG-IPs (Figure 2). All the *m/z* values of peptide features present in mαNavPAN-IPs and absent in mIgG-IPs were then selected and searched against theoretical *m/z* values of phosphorylated and unphosphorylated Nav1.5 peptides using a 20 ppm mass tolerance. Mass-matched peptide features corresponding to putative phosphorylated Nav1.5 peptides were filtered based upon several quality criteria as described in **Materials and Methods** and Figure 2, and the remaining peptide features (a total of 68) were selected for subsequent fragmentation in data-driven high-resolution MS2 analyses.

Mapping of Native Cardiac Nav1.5 Phosphorylation Sites

With the aim of identifying the basal *in situ* phosphorylation sites on the cardiac Nav1.5 α subunit protein, manual interpretations of MS2 spectra exhibiting possible phosphorylation(s) from the initial low-resolution MS2 analyses of the mαNavPAN-IPs were first undertaken. In these data-dependent analyses, two peptides were sequenced and annotated by the Mascot program as singly and doubly phosphorylated Nav1.5 peptides. In the triply charged, singly phosphorylated Nav1.5 peptide, AL(pS)AVSVLTSALEELEESHR (amino acids 662 to 681), the presence of masses of specific fragment ions containing (or not) a phosphate group unambiguously enabled the assignment of the phosphorylation site to serine-664 (pS664) (Table 2). Spectral annotation for the doubly phosphorylated Nav1.5 peptide, AL(pS)AV(pS)VLTSALEELEESHRK (amino acids 662 to 682), resulted in the identification of an additional phosphoserine at position 667 (pS667) (Table 2). The corresponding representative MS2 spectra of these phosphopeptides, as well as the percentage of maximum intensities of the site-discriminating ions allowing phosphorylation

site assignments, are presented in the Supplemental Figures and Table 2, respectively. Descriptions of all detected supporting ions are given in the Supplemental Tables.

To generate a comprehensive phosphorylation map of the cardiac Nav1.5 α subunit, a label-free comparative and data-driven phosphoproteomic strategy was exploited from the cardiac mαNavPAN-IPs and mIgG-IPs as described above and in Figure 2. Of the 68 peptide features selected for fragmentation and high-resolution MS2 analyses (see Figure 2), 15 corresponded to singly or doubly phosphorylated Nav1.5 peptides (Table 2). Annotation of 12 of these phosphopeptides unambiguously allowed the identification of 7 additional serine phosphorylation sites at positions 457, 460, 483, 484, 497, 510 and 571 (Table 2 and Supplemental Figures). As an example, spectral analysis of the singly phosphorylated Nav1.5 peptide, GVDTVSRS(pS)LEMSPLAPVTNHER (amino acids 452 to 474), enabled the assignment of the phosphorylation site to serine-460 (pS460) (Figure 3). The corresponding triply charged precursor ion was observed at *m/z* 854.739 with a mass error of −0.23 ppm as compared with the theoretical *m/z* 854.7388 (see left inset of Figure 3), and the most prominent ion in the collisionally induced tandem mass spectrum is the triply charged $[M + 3H - H_3PO_4]^{3+}$ species at *m/z* 822.079 characteristic of a neutral loss of phosphoric acid. Unambiguous assignment to serine-460 was afforded by the presence of the unphosphorylated b_8^{1+} (right inset of Figure 3), y_{12}^{1+} and y_{12}^{2+}, along with the phosphorylated b_9^{1+} and y_{17}^{2+} site-discriminating (or supporting) ions. Additionally, although determination of the exact site(s) of phosphorylation could not be made, analyses of 3 additional Nav1.5 phosphopeptide spectra (from high- or low-resolution data-driven MS2 analyses) supported the assignments of pS36, pT38, pS39 and/or pS42 as well as of pS524 and/or pS525 as sites of phosphorylation (Table 2 and Supplemental Figures). Calculated mass errors, confirmation of charge states (and percentages of maximum intensities for low-resolution MS2 spectra) of all detected site-discriminating and supporting ions are given in the Supplemental Tables.

Figure 4 illustrates the locations of the 11 phosphorylated residues identified. With the exception of one residue located in the cytoplasmic N-terminus (pS36, pT38, pS39 and/or pS42), all the phosphorylation sites identified are clustered in the first intracellular linker loop. No phosphosites were identified in the second and third intracellular linker loops or in the cytoplasmic C-terminus, although multiple non-modified peptides from these regions were detected (see Figure 1C).

Comparison of Mass Spectrometry-Identified and Predicted Nav1.5 Phosphorylation Sites

The *in situ* phosphorylation map of the cardiac Nav1.5 α subunit identified here using LC-MS/MS analyses was compared directly to phosphorylation site predictions obtained from widely used computer algorithms. Five distinct algorithms (Scansite[37], Phosphosite[38], NetPhos 2.0[39], DISPHOS[40] and NetPhosK 1.0[41]) were chosen based on the methods used for predictions ranging from simple consensus patterns to more advanced machine-learning algorithms. Interestingly, these algorithms did not reliably predict the pattern of *in situ* cardiac Nav1.5 phosphorylation sites observed experimentally. Indeed, as illustrated in Figure 5, only one of the (15) *in situ* phosphorylation site (pS525) identified here was predicted by all algorithms. The other *in situ* phosphorylation sites identified experimentally were either not predicted at all (pS667), or were predicted by one (pT38, pS510), two (pS36, pS39, pS42, pS524, pS664), three (pS457, pS497) or four (pS460, pS483, pS484) of the algorithms used. Interestingly, the algorithms also predicted a rather large number of other phosphorylation sites on the Nav1.5 protein that were not identified experimentally. NetPhos 2.0 and NetPhosK 1.0, for example, predicted a total of 121 and 144 phosphorylation sites, respectively, on the mouse Nav1.5 protein.

Discussion

The results presented here represent the first MS-based analysis of native cardiac Nav channels. In addition to identifying several components of cardiac Nav channel complexes by LC-MS/MS analyses, the phosphoproteomic approach developed and exploited here provides the first *in situ* basal phosphorylation map of the cardiac Nav1.5 α subunit and demonstrates that native cardiac Nav1.5 channels are highly phosphorylated. Whereas only two phosphorylated serines were detected using conventional data-dependent MS analyses, the use of the label-free comparative and data-driven phosphoproteomic strategy allowed the identification of nine additional phosphorylation sites on the native cardiac Nav1.5 protein, demonstrating the sensitivity and the effectiveness of the methodologies developed.

Mass Spectrometry-Based Identification of Native Cardiac Nav Channel Complexes

The immunoprecipitation approach for purifying native Nav channel complexes from adult mouse ventricles is efficient, and enabled the identification of several components of native cardiac Nav channels by LC-MS/MS analyses. In addition to the Nav1.5 α subunit, which is the main cardiac Nav α subunit[3, 4] and the most abundant protein identified in the IP, three other Nav α subunits, Nav1.3, Nav1.4 and Nav1.7, were also detected. Although much less abundant than Nav1.5 (Table 1), the presence of these other Nav α subunits is interesting in light of previous studies suggesting roles for neuronal Nav channel α subunits, including Nav1.1, Nav1.3 and Nav1.6 in coupling electrical excitation to contraction in the transverse tubules of cardiomyocytes[42]. It is certainly also possible, however, that these Nav α subunits are part of Nav channel complexes expressed in other cell types present in the heart, such as fibroblasts[43], neuronal[44] and/or endothelial[45] cells. Alternative experimental approaches will need to be exploited to define the physiological roles of these Nav α subunits in the myocardium. In addition to Nav α subunits, several previously identified Nav associated/regulatory proteins[3, 4], including calmodulin, the δ, β and γ subunits of Ca^{2+}/Calmodulin-dependent protein Kinase II (CamKIIδ, CamKIIβ, CamKIIγ) and intracellular Fibroblast Growth Factor 13 (FGF13)[36] were also identified.

Mass Spectrometry-Based Identification of Native Cardiac Nav1.5 α Subunit Phosphorylation Sites

The phosphoproteomic analyses here revealed unexpected complexity in the numbers and distributions of *in situ* basal phosphorylation sites on the Nav1.5 α subunit protein. A total of eleven phosphorylation sites on the native mouse ventricular Nav1.5 protein were identified, which compares in magnitude with the number (nine) of Nav1.5 phosphorylation sites previously identified in the literature[6, 11, 12, 46–48]. Interestingly, however, among the eleven native phosphorylation sites identified here, only four, serines-484[47], -525[6], -571[12] and -664[47] were suggested previously based on *in vitro* phosphorylation site analyses and/or predictions based upon consensus phosphorylation sequences. In this regard, it is particularly interesting to note that the five commonly used phosphorylation site prediction algorithms, including the cutting-edge NetPhosK 1.0[41], did not accurately predict *in situ* phosphorylation sites on the native Nav1.5 protein. Collectively, the available algorithms demonstrated low accuracy and poor prediction rankings for the majority of the MS-identified *in situ* phosphorylation sites on mouse ventricular Nav1.5, together with high sensitivity for numerous phosphorylation sites not detected *in situ*. Consistent with previous reports[13–15], therefore, the results presented here clearly suggest that the use of kinase consensus phosphorylation sites, as well as more advanced algorithms, to predict the numbers and locations of native protein phosphorylation sites has substantive limitations and, in addition, that MS-based proteomic analysis of native tissues is the approach of choice for identifying *in situ* and physiologically relevant phosphorylation sites.

With the exception of one residue located in the cytoplasmic N-terminus, all of the phosphorylation sites identified here are clustered in the first intracellular linker loop of Nav1.5. These findings are consistent with previous studies on cardiac[6–8, 49] and neuronal[13, 14, 50] Na^+ channels, suggesting a critical and highly-conserved role for this region in phosphorylation-dependent channel regulation. Using two-dimensional phosphopeptide mapping, for example, two *in vitro* PKA phosphorylation sites (at serines-525 and -528) have previously been identified on the Nav1.5 protein[6]. In addition, functional studies revealed that phosphorylation at these sites enhances channel trafficking to the cell surface and increases Na^+ current densities[7, 8]. Depending on the cellular model used, however, PKA has been reported to cause diverse effects on cardiac Na^+ channels[51, 52], suggesting that additional phosphorylation sites are present and can cause additional functional effects. Several of the other phosphorylation sites identified here, specifically serines-460, -483, -484, -510, -571 and -664, also correspond (in addition to serine-525) to predicted PKA phosphorylation sites (NetPhosK 1.0 predictions) and represent, therefore, good candidates for multisite phosphorylation-dependent regulation by PKA. Nav channel phosphorylation and regulation by the Serum and Glucocorticoid inducible Kinases (SGK) have also been suggested to modify residues in the first intracellular linker loop, specifically at serines-484 and -664[47]. Phosphorylation of serine-571 (as also identified *in situ*) in the first intracellular linker loop has previously been suggested to mediate the regulation of Nav1.5 channels by the Ca^{2+}/Calmodulin-dependent protein Kinase II under basal conditions[12], whereas subsequent analyses have suggested roles for phosphorylation of serine-516 and threonine-594 (not found here) under pathological conditions[11].

To determine if the *in situ* basal phosphorylation sites identified here on mouse cardiac Nav1.5 are conserved across species, the rat and human Nav1.5 proteins were aligned with the mouse sequence (Figure 6). To extend the comparison to other Nav α subunits, the amino acid sequences of Nav1.1 through Nav1.9 were also aligned and the positions of the corresponding serines and threonines were compared (Figure 6). The Nav protein sequences in Figure 6, except Nav1.1 and Nav1.2, are mouse. The rat Nav1.1 and Nav1.2 sequences were aligned with mouse Nav1.5 to allow direct comparison of the phosphorylation sites identified here with the native phosphorylation sites previously identified on rat brain Nav1.2 (and Nav1.1) using similar mass spectrometric analyses[13]. It is noteworthy that all of the phosphorylation sites identified on the rat brain Nav1.2 and Nav1.1 proteins[13] are conserved in the orthologous mouse sequences (not illustrated).

These analyses revealed that, with the exception of phosphoserine-39, all of the basal phosphorylation sites identified in the present study on mouse cardiac Nav1.5 are conserved in the rat and human Nav1.5 proteins (Figure 6). In contrast, only one of the (15) phosphorylation sites, phosphoserine-525, on mouse cardiac Nav1.5 was also identified (phosphoserine-554) on rat brain Nav1.2[13] (Figure 6). Interestingly, serine-525 in cardiac Nav1.5[6–8] and serine-554 in brain Nav1.2[53] have both been previously suggested to be PKA targets. All of the other (28) phosphorylated serines and threonines identified on mouse Nav1.5 and brain Nav1.2[13] were either not present in the counterpart sequence (19 of them), or when present (9 of them), were surrounded by different amino acids (Figure 6), which could impact the likelihood of phosphorylation at these positions. As an illustration of these observations, the mouse cardiac Nav1.5 phosphoserine-510 aligns with a phenylalanine residue on the rat Nav1.2 protein (Figure 6). On the contrary, although the Nav1.5 phosphoserine-664 is present across all Nav homologues (except Nav1.4), the amino acids surrounding this serine in each of the Nav proteins are distinct (Figure 6).

With the identification of eleven, including eight novel, *in situ* phosphorylation sites, the results here demonstrate high basal phosphorylation of the mouse cardiac Nav1.5 protein,

suggesting additional levels of complexity involved in the *in vivo* regulation of myocardial Nav1.5-encoded channel expression and functioning. It is important to also note here, however, that these proteomic data provide no direct information regarding protein function, and that it will be necessary, therefore, to define the functional roles of these newly identified phosphorylation sites, as well as the kinases and phosphatases involved in controlling phosphorylation at these sites in native cells, using alternative experimental approaches.

Advantages and Limitations of the Mass Spectrometry Approaches Used

The combined use of immunoaffinity purification from native tissue and label-free comparative and data-driven phosphoproteomic analyses allowed the identification of the basal *in situ* phosphorylation sites on the Nav1.5 protein immunoprecipitated from adult mouse hearts with no *a priori* knowledge or hypotheses. First and foremost, the use of channel proteins purified from native tissue offered the clear advantage of identifying *in situ* phosphorylation sites directly. Second, the application of the label-free comparative and data-driven mass spectrometry approaches here allowed us to circumvent the sensitivity limitations inherent in mass spectrometry[20, 22, 27], which generally proscribe the detection of low-abundance phosphorylated peptides[24, 26, 28]. Indeed, contrary to more conventional data-dependent (or intensity-driven) analyses, where only the most intense peptide signals are triggered for MS2 acquisitions (which here allowed the identification of only two Nav1.5 phosphorylation sites), the data-driven analyses enabled us to acquire MS2 spectra on a comprehensive set of selected lower-abundance phosphorylated Nav1.5 peptides, thereby increasing the number of Nav1.5 phosphorylation sites identified to eleven. Further enrichment was realized using label-free comparative analysis followed by *in silico* mass-matching with theoretical phosphorylated Nav1.5 peptides which provided us with a list of all possible phosphorylated Nav1.5 peptides from the mouse cardiac tissue sample analyzed. Another clear advantage of the phosphoproteomic analyses developed here is the use of high mass resolution MS1 and MS2 analyses which supported high-confidence spectral annotations. Based on the results here, future studies focused on using this in-depth and quantitative phosphoproteomic approach to identify kinase-specific phosphorylation sites and to compare the phosphorylation status of Nav1.5 and other myocardial proteins under different physiological and pathophysiological conditions are certainly warranted and will be of considerable interest.

The use of MS-based proteomic approaches, nonetheless, also presents several caveats. Technical limitations associated with the lability of phosphorylation modifications, or in other words, with our inability to maintain these sites intact during the numerous steps involved in immunoaffinity purification and protein digestion are highly probable. As a consequence, it is important to keep in mind that the absence of detection of a phosphorylated peptide does not necessarily mean that phosphorylation of this site is not present *in situ*. This might be the case, for example, of phosphorylation of serine-1503 by PKC which has previously been shown to reduce Na^+ channel trafficking and current densities and to alter channel steady-state inactivation[48, 54]. It is certainly possible that the regulation of cardiac Nav1.5-encoded channels by PKC under basal conditions is minor and/or only occurs in response to specific physiological or pathophysiological stimuli. Similarly, phosphorylation of tyrosine-1498, which has previously been suggested to mediate regulation of Nav1.5 channels by the Src family tyrosine kinase Fyn in HEK-293 cells[46], has not been detected in the MS analyses here. Beyond the various technical limitations described above, multiple biological reasons could also account for this absence of detection, such as differences in species or cellular models. Finally, it is important to consider that the phosphorylation sites identified in the present study, with the exception of the phosphorylation sites identified from doubly phosphorylated peptides, do not necessarily

originate from a single Nav1.5 α subunit, but could also belong to different pools of Nav1.5 molecules, localized, for example, in distinct subcellular compartments[12, 55]. Taken together, the results presented here highlight an unexpected complexity in the extent and the distribution of *in situ* phosphorylation sites on the cardiac Nav1.5 channel α subunit and emphasize the importance of developing such *in situ* analyses for the identification of physiologically or pathophysiologically relevant phosphorylation sites.

Supplementary Material

Refer to Web version on PubMed Central for supplementary material.

Acknowledgments

The authors acknowledge financial support provided to their laboratories by the Agence Nationale de la Recherche (ANR-08-GENO-006 to JM), the Marie Curie 7th Framework Program of the European Commission (NavEx-256397 to CM), the Fondation pour la Recherche Médicale (DCV20076409253 to FC) and the National Institutes of Health (RR00954 to RRT, UL1 RR024992 to RRT and HL-034161 to JMN). In addition, the expert technical assistance of Petra Erdmann-Gilmore and Alan E Davis is gratefully acknowledged. We would also like to thank Dr. Hélène Rogniaux from the Biopolymers, Structural Biology Platform (BIBS platform, INRA UR1268 Biopolymers Interactions Assemblies, F-44316 Nantes) for the in-gel mass spectrometric analyses.

Abbreviations

IP	Immunoprecipitation
LC-MS/MS	Liquid Chromatography-tandem Mass Spectrometry
MS	Mass Spectrometry
MS1	Mass spectrum of precursor ions
MS2	MS/MS or tandem Mass Spectrometry
mαNavPAN	Anti-Nav α subunit monoclonal antibody
mIgG	Mouse Immunoglobulin G
Nav α subunit	Voltage-gated Na^+ (Nav) channel pore-forming (α) subunit

References

1. Nerbonne JM, Kass RS. Molecular physiology of cardiac repolarization. Physiol Rev. 2005; 85(4): 1205–1253. [PubMed: 16183911]
2. Remme CA, Bezzina CR. Sodium channel (dys)function and cardiac arrhythmias. Cardiovasc Ther. 2010; 28(5):287–294. [PubMed: 20645984]
3. Abriel H. Cardiac sodium channel Na(v)1.5 and interacting proteins: Physiology and pathophysiology. J Mol Cell Cardiol. 2010; 48(1):2–11. [PubMed: 19744495]
4. Rook MB, Evers MM, Vos MA, Bierhuizen MF. Biology of cardiac sodium channel Nav1.5 expression. Cardiovasc Res. 2012; 93(1):12–23. [PubMed: 21937582]
5. Matsuda JJ, Lee H, Shibata EF. Enhancement of rabbit cardiac sodium channels by beta-adrenergic stimulation. Circ Res. 1992; 70(1):199–207. [PubMed: 1309315]
6. Murphy BJ, Rogers J, Perdichizzi AP, Colvin AA, Catterall WA. cAMP-dependent phosphorylation of two sites in the alpha subunit of the cardiac sodium channel. J Biol Chem. 1996; 271(46):28837–28843. [PubMed: 8910529]
7. Zhou J, Shin HG, Yi J, Shen W, Williams CP, Murray KT. Phosphorylation and putative ER retention signals are required for protein kinase A-mediated potentiation of cardiac sodium current. Circ Res. 2002; 91(6):540–546. [PubMed: 12242273]

8. Zhou J, Yi J, Hu N, George AL Jr, Murray KT. Activation of protein kinase A modulates trafficking of the human cardiac sodium channel in Xenopus oocytes. Circ Res. 2000; 87(1):33–38. [PubMed: 10884369]

9. Maltsev VA, Reznikov V, Undrovinas NA, Sabbah HN, Undrovinas A. Modulation of late sodium current by Ca2+, calmodulin, and CaMKII in normal and failing dog cardiomyocytes: similarities and differences. Am J Physiol Heart Circ Physiol. 2008; 294(4):H1597–H1608. [PubMed: 18203851]

10. Wagner S, Dybkova N, Rasenack EC, Jacobshagen C, Fabritz L, Kirchhof P, Maier SK, Zhang T, Hasenfuss G, Brown JH, Bers DM, Maier LS. Ca2+/calmodulin-dependent protein kinase II regulates cardiac Na+ channels. J Clin Invest. 2006; 116(12):3127–3138. [PubMed: 17124532]

11. Ashpole NM, Herren AW, Ginsburg KS, Brogan JD, Johnson DE, Cummins TR, Bers DM, Hudmon A. Ca2+/Calmodulin-dependent Protein Kinase II (CaMKII) Regulates Cardiac Sodium Channel NaV1.5 Gating by Multiple Phosphorylation Sites. J Biol Chem. 2012; 287(24):19856–19869. [PubMed: 22514276]

12. Hund TJ, Koval OM, Li J, Wright PJ, Qian L, Snyder JS, Gudmundsson H, Kline CF, Davidson NP, Cardona N, Rasband MN, Anderson ME, Mohler PJ. A beta(IV)-spectrin/CaMKII signaling complex is essential for membrane excitability in mice. J Clin Invest. 2010; 120(10):3508–3519. [PubMed: 20877009]

13. Berendt FJ, Park KS, Trimmer JS. Multisite phosphorylation of voltage-gated sodium channel alpha subunits from rat brain. J Proteome Res. 2010; 9(4):1976–1984. [PubMed: 20131913]

14. Cerda O, Baek JH, Trimmer JS. Mining recent brain proteomic databases for ion channel phosphosite nuggets. J Gen Physiol. 2011; 137(1):3–16. [PubMed: 21149544]

15. Wisniewski JR, Nagaraj N, Zougman A, Gnad F, Mann M. Brain phosphoproteome obtained by a FASP-based method reveals plasma membrane protein topology. J Proteome Res. 2010; 9(6):3280–3289. [PubMed: 20415495]

16. Park KS, Mohapatra DP, Misonou H, Trimmer JS. Graded regulation of the Kv2.1 potassium channel by variable phosphorylation. Science. 2006; 313(5789):976–979. [PubMed: 16917065]

17. Yang JW, Vacher H, Park KS, Clark E, Trimmer JS. Trafficking-dependent phosphorylation of Kv1.2 regulates voltage-gated potassium channel cell surface expression. Proc Natl Acad Sci U S A. 2007; 104(50):20055–20060. [PubMed: 18056633]

18. Yan J, Olsen JV, Park KS, Li W, Bildl W, Schulte U, Aldrich RW, Fakler B, Trimmer JS. Profiling the phospho-status of the BKCa channel alpha subunit in rat brain reveals unexpected patterns and complexity. Mol Cell Proteomics. 2008; 7(11):2188–2198. [PubMed: 18573811]

19. Nilsson CL. Advances in quantitative phosphoproteomics. Anal Chem. 2012; 84(2):735–746. [PubMed: 22043985]

20. America AH, Cordewener JH. Comparative LC-MS: a landscape of peaks and valleys. Proteomics. 2008; 8(4):731–749. [PubMed: 18297651]

21. Chen ZW, Fuchs K, Sieghart W, Townsend RR, Evers AS. Deep amino acid sequencing of native brain GABAA receptors using high-resolution mass spectrometry. Mol Cell Proteomics. 2012; 11(1):M111 011445.

22. Neubert H, Bonnert TP, Rumpel K, Hunt BT, Henle ES, James IT. Label-free detection of differential protein expression by LC/MALDI mass spectrometry. J Proteome Res. 2008; 7(6):2270–2279. [PubMed: 18412385]

23. Nittis T, Guittat L, Leduc RD, Dao B, Duxin JP, Rohrs H, Townsend RR, Stewart SA. Revealing novel telomere proteins using in vivo crosslinking,tandem affinity purification and label-free quantitative LC-FTICR-MS. Mol Cell Proteomics. 2010

24. Carr SA, Huddleston MJ, Annan RS. Selective detection and sequencing of phosphopeptides at the femtomole level by mass spectrometry. Anal Biochem. 1996; 239(2):180–192. [PubMed: 8811904]

25. Marionneau C, Townsend RR, Nerbonne JM. Proteomic analysis highlights the molecular complexities of native Kv4 channel macromolecular complexes. Semin Cell Dev Biol. 2011; 22(2):145–152. [PubMed: 20959143]

26. Meyer MR, Lichti CF, Townsend RR, Rao AG. Identification of in vitro autophosphorylation sites and effects of phosphorylation on the Arabidopsis CRINKLY4 (ACR4) receptor-like kinase

intracellular domain: insights into conformation, oligomerization, and activity. Biochemistry. 2011; 50(12):2170–2186. [PubMed: 21294549]

27. Wilm M, Neubauer G, Mann M. Parent ion scans of unseparated peptide mixtures. Anal Chem. 1996; 68(3):527–533. [PubMed: 8712361]
28. Zappacosta F, Collingwood TS, Huddleston MJ, Annan RS. A quantitative results-driven approach to analyzing multisite protein phosphorylation: the phosphate-dependent phosphorylation profile of the transcription factor Pho4. Mol Cell Proteomics. 2006; 5(11):2019–2030. [PubMed: 16825185]
29. Vassilev PM, Scheuer T, Catterall WA. Identification of an intracellular peptide segment involved in sodium channel inactivation. Science. 1988; 241(4873):1658–1661. [PubMed: 2458625]
30. Schneider C, Newman RA, Sutherland DR, Asser U, Greaves MF. A one-step purification of membrane proteins using a high efficiency immunomatrix. J Biol Chem. 1982; 257(18):10766–10769. [PubMed: 6955305]
31. Yu YQ, Gilar M, Gebler JC. A complete peptide mapping of membrane proteins: a novel surfactant aiding the enzymatic digestion of bacteriorhodopsin. Rapid Commun Mass Spectrom. 2004; 18(6):711–715. [PubMed: 15052583]
32. Keller A, Nesvizhskii AI, Kolker E, Aebersold R. Empirical statistical model to estimate the accuracy of peptide identifications made by MS/MS and database search. Anal Chem. 2002; 74(20):5383–5392. [PubMed: 12403597]
33. Nesvizhskii AI, Keller A, Kolker E, Aebersold R. A statistical model for identifying proteins by tandem mass spectrometry. Anal Chem. 2003; 75(17):4646–4658. [PubMed: 14632076]
34. Strohalm M, Kavan D, Novak P, Volny M, Havlicek V. mMass 3: a cross-platform software environment for precise analysis of mass spectrometric data. Anal Chem. 2010; 82(11):4648–4651. [PubMed: 20465224]
35. Marionneau C, LeDuc RD, Rohrs HW, Link AJ, Townsend RR, Nerbonne JM. Proteomic analyses of native brain K(V)4.2 channel complexes. Channels (Austin). 2009; 3(4):284–294. [PubMed: 19713751]
36. Wang C, Hennessey JA, Kirkton RD, Graham V, Puranam RS, Rosenberg PB, Bursac N, Pitt GS. Fibroblast growth factor homologous factor 13 regulates Na+ channels and conduction velocity in murine hearts. Circ Res. 2011; 109(7):775–782. [PubMed: 21817159]
37. Obenauer JC, Cantley LC, Yaffe MB. Scansite 2.0: Proteome-wide prediction of cell signaling interactions using short sequence motifs. Nucleic Acids Res. 2003; 31(13):3635–3641. [PubMed: 12824383]
38. Hornbeck PV, Chabra I, Kornhauser JM, Skrzypek E, Zhang B. PhosphoSite: A bioinformatics resource dedicated to physiological protein phosphorylation. Proteomics. 2004; 4(6):1551–1561. [PubMed: 15174125]
39. Blom N, Gammeltoft S, Brunak S. Sequence and structure-based prediction of eukaryotic protein phosphorylation sites. J Mol Biol. 1999; 294(5):1351–1362. [PubMed: 10600390]
40. Iakoucheva LM, Radivojac P, Brown CJ, O'Connor TR, Sikes JG, Obradovic Z, Dunker AK. The importance of intrinsic disorder for protein phosphorylation. Nucleic Acids Res. 2004; 32(3):1037–1049. [PubMed: 14960716]
41. Blom N, Sicheritz-Ponten T, Gupta R, Gammeltoft S, Brunak S. Prediction of post-translational glycosylation and phosphorylation of proteins from the amino acid sequence. Proteomics. 2004; 4(6):1633–1649. [PubMed: 15174133]
42. Maier SK, Westenbroek RE, Schenkman KA, Feigl EO, Scheuer T, Catterall WA. An unexpected role for brain-type sodium channels in coupling of cell surface depolarization to contraction in the heart. Proc Natl Acad Sci U S A. 2002; 99(6):4073–4078. [PubMed: 11891345]
43. Li GR, Sun HY, Chen JB, Zhou Y, Tse HF, Lau CP. Characterization of multiple ion channels in cultured human cardiac fibroblasts. PLoS One. 2009; 4(10):e7307. [PubMed: 19806193]
44. Yoo S, Dobrzynski H, Fedorov VV, Xu SZ, Yamanushi TT, Jones SA, Yamamoto M, Nikolski VP, Efimov IR, Boyett MR. Localization of Na+ channel isoforms at the atrioventricular junction and atrioventricular node in the rat. Circulation. 2006; 114(13):1360–1371. [PubMed: 16966585]
45. Andrikopoulos P, Fraser SP, Patterson L, Ahmad Z, Burcu H, Ottaviani D, Diss JK, Box C, Eccles SA, Djamgoz MB. Angiogenic functions of voltage-gated Na+ Channels in human endothelial

cells: modulation of vascular endothelial growth factor (VEGF) signaling. J Biol Chem. 2011; 286(19):16846–16860. [PubMed: 21385874]

46. Ahern CA, Zhang JF, Wookalis MJ, Horn R. Modulation of the cardiac sodium channel NaV1.5 by Fyn, a Src family tyrosine kinase. Circ Res. 2005; 96(9):991–998. [PubMed: 15831816]
47. Boehmer C, Wilhelm V, Palmada M, Wallisch S, Henke G, Brinkmeier H, Cohen P, Pieske B, Lang F. Serum and glucocorticoid inducible kinases in the regulation of the cardiac sodium channel SCN5A. Cardiovasc Res. 2003; 57(4):1079–1084. [PubMed: 12650886]
48. Murray KT, Hu NN, Daw JR, Shin HG, Watson MT, Mashburn AB, George AL Jr. Functional effects of protein kinase C activation on the human cardiac Na+ channel. Circ Res. 1997; 80(3): 370–376. [PubMed: 9048657]
49. Frohnwieser B, Chen LQ, Schreibmayer W, Kallen RG. Modulation of the human cardiac sodium channel alpha-subunit by cAMP-dependent protein kinase and the responsible sequence domain. J Physiol. 1997; 498(Pt 2):309–318. [PubMed: 9032680]
50. Rossie S, Catterall WA. Phosphorylation of the alpha subunit of rat brain sodium channels by cAMP-dependent protein kinase at a new site containing Ser686 and Ser687. J Biol Chem. 1989; 264(24):14220–14224. [PubMed: 2547790]
51. Chandra R, Chauhan VS, Starmer CF, Grant AO. beta-Adrenergic action on wild-type and KPQ mutant human cardiac Na+ channels: shift in gating but no change in Ca2+:Na+ selectivity. Cardiovasc Res. 1999; 42(2):490–502. [PubMed: 10533584]
52. Ono K, Fozzard HA, Hanck DA. Mechanism of cAMP-dependent modulation of cardiac sodium channel current kinetics. Circ Res. 1993; 72(4):807–815. [PubMed: 8383015]
53. Rossie S, Gordon D, Catterall WA. Identification of an intracellular domain of the sodium channel having multiple cAMP-dependent phosphorylation sites. J Biol Chem. 1987; 262(36):17530–17535. [PubMed: 2447073]
54. Hallaq H, Wang DW, Kunic JD, George AL Jr, Wells KS, Murray KT. Activation of protein kinase C alters the intracellular distribution and mobility of cardiac Na+ channels. Am J Physiol Heart Circ Physiol. 2012; 302(3):H782–H789. [PubMed: 22101522]
55. Petitprez S, Zmoos AF, Ogrodnik J, Balse E, Raad N, El-Haou S, Albesa M, Bittihn P, Luther S, Lehnart SE, Hatem SN, Coulombe A, Abriel H. SAP97 and dystrophin macromolecular complexes determine two pools of cardiac sodium channels Nav1.5 in cardiomyocytes. Circ Res. 2011; 108(3):294–304. [PubMed: 21164104]

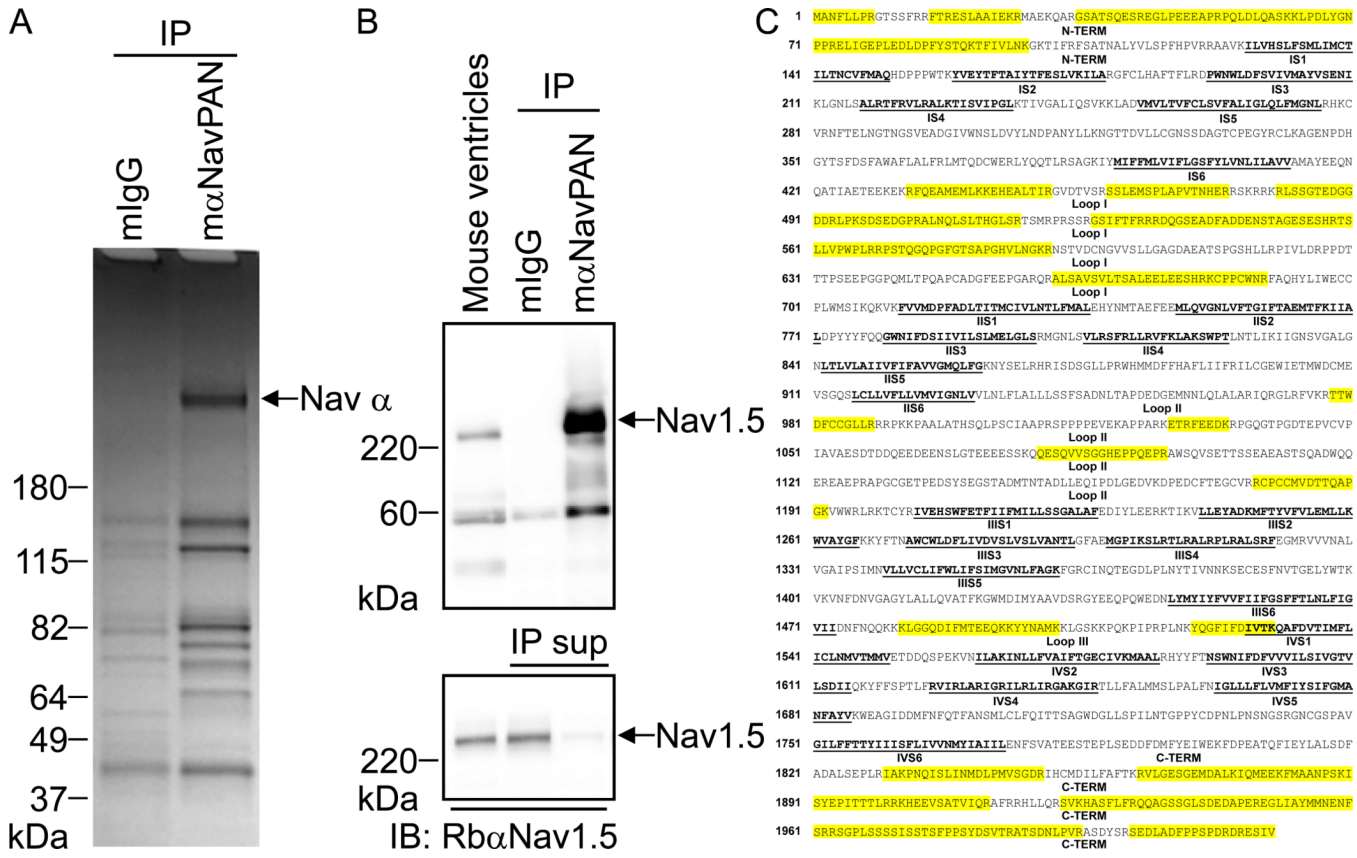

Figure 1.

Immunoprecipitation of cardiac Nav channel complexes. (**A**) Coomassie blue stained-gel of immunoprecipitated (IP) proteins from adult wild-type mouse cardiac ventricles with the anti-NavPAN monoclonal antibody (mαNavPAN, directed against all Nav α subunits) or with non-specific mouse immunoglobulin G (mIgG). Proteins running at the molecular weight corresponding to the Nav α subunits are clearly evident in the mαNavPAN-IP and were identified directly using in-gel LC-MS/MS analyses (data not shown). None of these Nav α subunits were detected in the control mIgG-IP. **(B)** Representative Western blot of mαNavPAN- and mIgG-IPs probed with an anti-Nav1.5 rabbit polyclonal antibody (RbαNav1.5). The Nav1.5 protein is clearly evident in the mαNavPAN-IP, but is absent in the control mIgG-IP. In the lower panel, the same amounts of the corresponding IP supernatants (IP sup) were analyzed, revealing that > 80% depletion of the Nav1.5 protein was achieved. (**C**) Amino acid sequence coverage obtained for the (mouse) Nav1.5 protein. Detected peptides are highlighted in yellow; transmembrane segments (S1–S6) in each domain (I–IV) are in bold and are underlined in black; and loops I, II and III correspond to the interdomains I–II, II–III and III–IV, respectively.

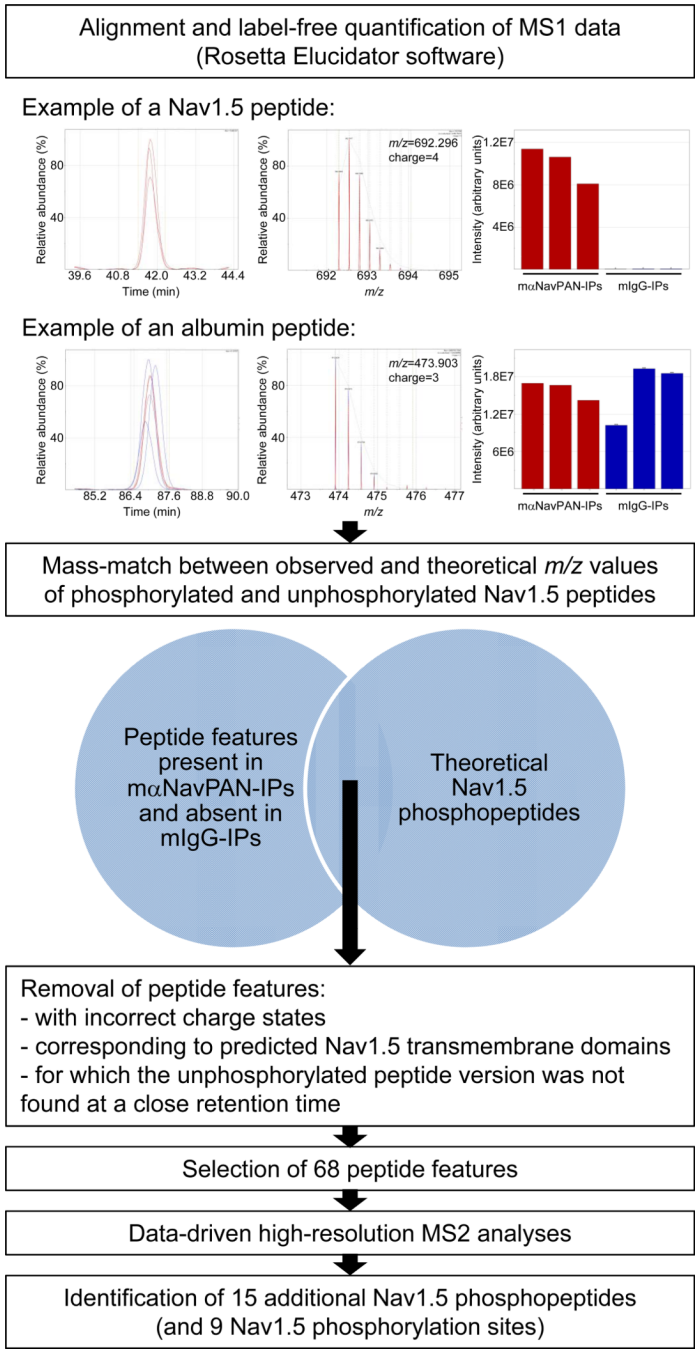

Figure 2.

Schematic flow diagram illustrating the label-free comparative and data-driven phosphoproteomic strategy used to identify *in situ* cardiac Nav1.5 phosphorylation sites. MS1 data obtained from high-resolution mass spectra of precursor ions from triplicate analyses of mαNavPAN- and mIgG-IPs were aligned (based upon *m/z* and retention times) and label-free quantified off-line using the Rosetta Elucidator software[22]. The ion chromatograms, isotope clusters and intensities of two annotated peptide features are illustrated. The Nav1.5 peptide is detected in the (triplicate) mαNavPAN-IPs, but is absent in the (triplicate) mIgG-IPs whereas the albumin peptide is equally represented in the mαNavPAN- and mIgG-IPs. The *m/z* values of peptide features present in mαNavPAN-IPs

and absent in mIgG-IPs were then searched against theoretical *m/z* values of phosphorylated and unphosphorylated Nav1.5 peptides using a 20 ppm mass tolerance. Mass-matched peptide features corresponding to putative phosphorylated Nav1.5 peptides were subsequently filtered based upon several quality criteria, and the remaining peptide features (a total of 68) were finally selected for fragmentation in data-driven high-resolution MS2 analyses. These analyses led to the identification of 15 additional Nav1.5 phosphopeptides and 9 Nav1.5 phosphorylation sites.

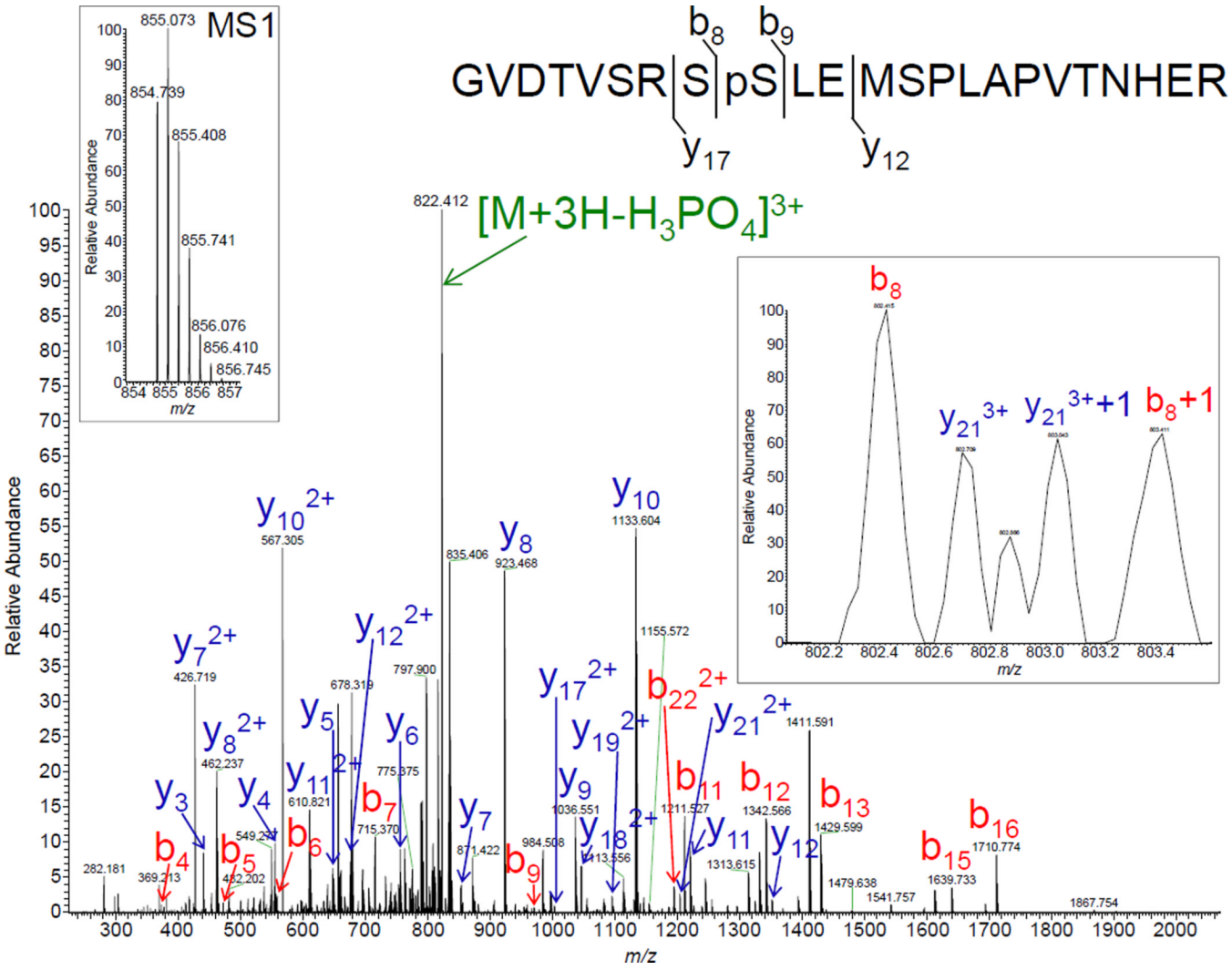

Figure 3.

Representative high-resolution tandem mass (MS2) spectrum of the singly phosphorylated Nav1.5 tryptic peptide demonstrating the phosphorylation of serine-460 (pS460). The triply charged singly phosphorylated Nav1.5 peptide at *m/z* 854.739 (left inset) was fragmented to produce a MS2 spectrum with y- (highlighted in blue) and b- (in red) ion series that describe the sequence NH2-GVDTVSRS(pS)LEMSPLAPVTNHER-COOH (amino acids 452–474). The most prominent ion in the MS2 spectrum is the triply charged $[M+3H-H_3PO_4]^{3+}$ species at *m/z* 822.079 (highlighted in green), characteristic of a neutral loss of phosphoric acid. The phosphorylation site was unambiguously assigned to serine-460 due to the presence of the unphosphorylated b_8^{1+} (right inset), y_{12}^{1+} and y_{12}^{2+}, along with the phosphorylated b_9^{1+} and y_{17}^{2+} site-discriminating (or supporting) ions. The charge state confirmations and the percentages of maximum intensities of site-discriminating ions are presented in Table 2, and the complete list of assigned ions is given in the Supplemental Table.

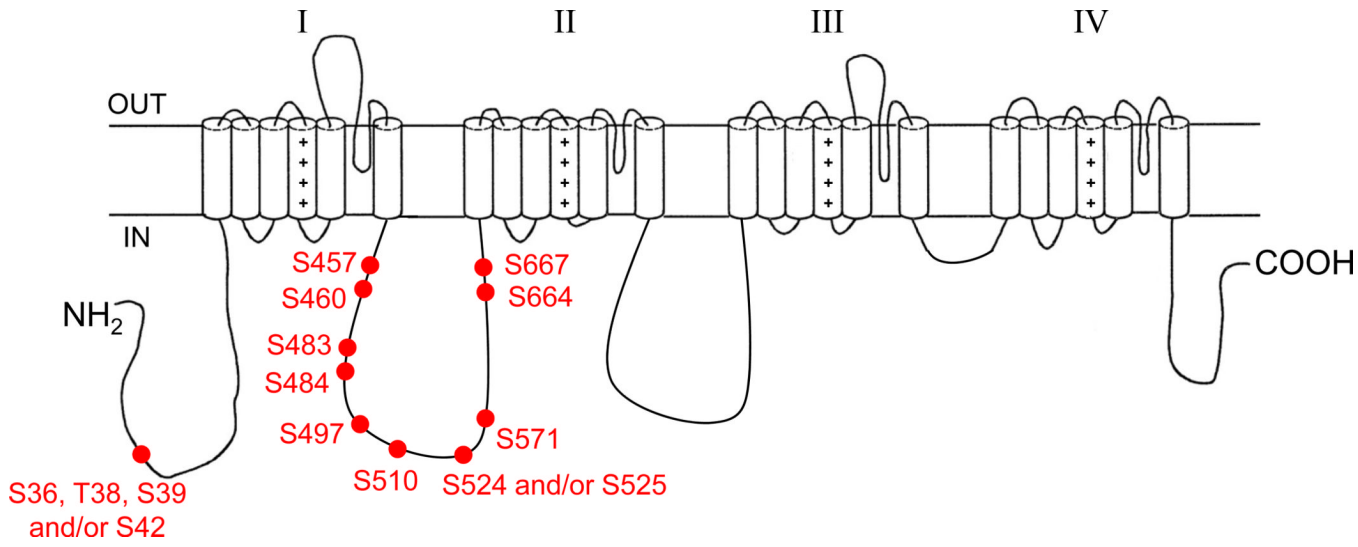

Figure 4.

Localization of MS-identified *in situ* phosphorylation sites on the mouse cardiac Nav1.5 α subunit protein. Four and two phosphorylation site locations are possible at amino acids 36 to 42 and 524 to 525, respectively. With the exception of one residue located in the cytoplasmic N-terminus (pS36, pT38, pS39 and/or pS42), all the phosphorylation sites identified are clustered in the first intracellular linker loop.

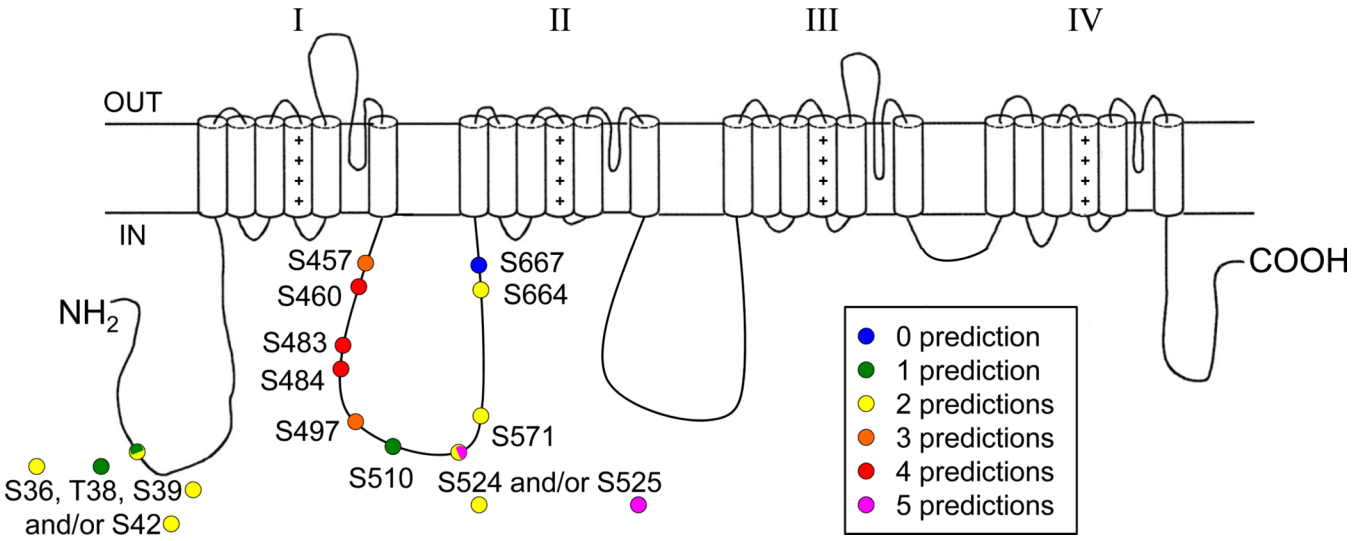

Figure 5.

Comparison of MS-identified and predicted Nav1.5 α subunit phosphorylation sites. The *in situ* phosphorylation sites identified here are color-coded to show the frequencies of representation in the predictions from five distinct algorithms (Scansite, Phosphosite, NetPhos 2.0, DISPHOS and NetPhosK 1.0).

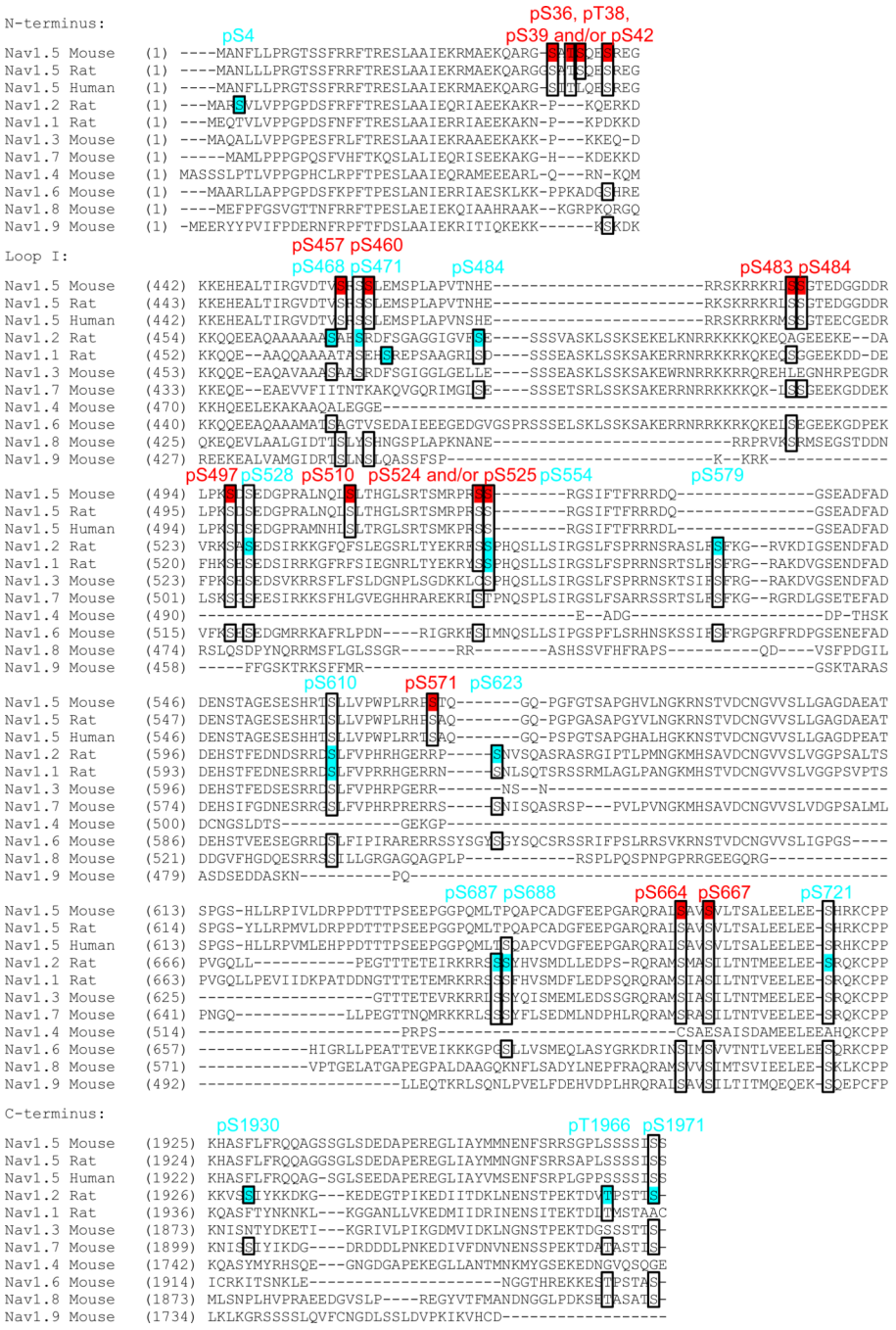

Figure 6.

Sequence alignment and conservation of phosphorylation sites across Nav channel homologues and species. The multiple amino acid sequence alignment was constructed using the ClustalW algorithm (from the Vector NTI 9.1.0 software, Invitrogen), and the following NCBI Reference Sequences were used: NP_067519.2 for mouse Nav1.5, NP_037257.1 for rat Nav1.5, NP_932173.1 for human Nav1.5, NP_036779.1 for rat Nav1.2, NP_110502.1 for rat Nav1.1, NP_061202.3 for mouse Nav1.3, NP_061340.2 for mouse Nav1.7, NP_573462.2 for mouse Nav1.4, NP_001070967.1 for mouse Nav1.6, NP_001192250.1 for mouse Nav1.8, and NP_036017.3 for mouse Nav1.9. Alignment results of portions of the N-terminus, loop I (interdomain I-II) and the C-terminus are shown

only. The native mouse cardiac Nav1.5 phosphorylation sites identified in the present study are highlighted in red, and compared directly with the native phosphorylation sites identified on the rat brain Nav1.2 (and Nav1.1) proteins[13] (in blue). The conservation of serines and threonines identified as *in situ* phosphorylation sites in the two studies is presented in boxes.

Table 1

Proteins identified in immunoprecipitated cardiac Nav channel complexes using LC-MS/MS[1]

Protein	Numbers of peptides: unique (total)	% Amino acid sequence coverage
Nav1.5	86 (298)	25%
Nav1.4	10 (31)	8%
Nav1.3	3 (13)	4%
Nav1.7	1 (6)	2%
Calmodulin	8 (27)	27%
CamKIIδ	24 (67)	35%
CamKIIβ	6 (55)	22%
CamKIIγ	9 (47)	25%
FGF13	1 (1)	6%

[1]The numbers of unique peptides, as well as the total numbers of peptides and the percent (%) amino acid sequence coverage, for each protein are presented. Scaffold peptide and protein probability scores were greater than 95%. None of the proteins listed were identified in the control immunoprecipitations. Abbreviations: Nav, voltage-gated Na^+ channel; LC-MS/MS, Liquid Chromatography-tandem Mass Spectrometry; CamKII, Ca^{2+}/Calmodulin-dependent protein Kinase II; FGF13, Fibroblast Growth Factor 13.

Table 2

Phosphorylation sites, phosphopeptides and site-discriminating ions identified in immunoprecipitated cardiac Nav1.5 channel a subunits using LC-MS/MS[1]

Phosphorytion site	Mass resolution	Phosphopeptide sequence	*m/z* (charge)	b ion	Phosphorylated b ion	y ion	Phosphorylated y ion
pS36, pT38, pS39 and/or pS42	High MS2	35-GSATSQESREGLPEEEAPRPQLDLQASK	1030.817 (+3)	b (--)	b (--)	y18 (+2, 1.6)	y (--)
pS36, T38, S39 and/or S42	High MS2	35-GSATSQESREGLPEEEAPRPQLDLQASK	773.364 (+4)	b (--)	b12 (+1, 60.9) b12 (+2, 10.7)	y16 (+2, 100) y16 (+3, 41.0)	y (--)
pS457 + pS460	High MS2	452-GVDTV(pS)RS(pS)LEMSPLAPVTNHER	881.394 (+3)	b5 (−, 0.1)	b7 (+1, 1) b8 (−, 0.1)	y14 (+2, 1.1)	y17 (+2, 0.1)
pS460	High MS2	452-GVDTVSRS(pS)LEMSPLAPVTNHER	854.738 (+3)	b8 (+1, 3.6)	b9 (+1, 0.7)	y14 (--)	y15 (--)
pS483	High MS2	481-RL(pS)SGTEDGGDDRLPK	594.938 (+3)	b2 (+1, 3.1)	b3 (--)	y13 (+2, 2.2)	y14 (−, 0.4)
pS484	High MS2	482-LS(pS)GTEDGGDDRLPK	542.905 (+3)	b2 (−, 23.2)	b3 (−, 2.7)	y12 (+2, 30.9)	y13 (+2, 27.5)
pS484	High MS2	482-LS(pS)GTEDGGDDRLPK	813.854 (+2)	b2 (--)	b3 (--)	y12 (+1, 9.8) y12 (+2, 28.4)	y13 (−, 0.7)
pS484	High MS2	482-LS(pS)GTEDGGDDRLPKSDSEDGPR	824.017 (+3)	b2 (--)	b3 (--)	y20 (+2, 25.3) y20 (+3, 9.8)	y21 (+3, 6.4)
pS483 + pS484	High MS2	481-RL(pS)(pS)GTEDGGDDRLPK	621.594 (+3)	b2 (+1, 23.2)	b3 (--)	y12 (+2, 6.9)	y13 (+2, 6.7) y14 (+2, 0.2)
pS483 + pS484	High MS2	480-KRL(pS)(pS)GTEDGGDDRLPK	664.292 (+3)	b3 (−, 0.4)	b4 (−, 0.4)	y12 (+2, 5.8)	y13 (+2, 1.2)
pS497	High MS2	482-LSSGTEDGGDDRLPK(pS)DSEDGPR	824.017 (+3)	b15 (--)	b16 (--)	y7 (+1, 29.1)	y8 (−, 10.8)
pS510	High MS2	505-ALNQL(pS)LTHGLSR	497.255 (+3)	b5 (+1, 7.9)	b6 (--)	y7 (+2, 3.3)	y8 (−, 0.2)
pS510	High MS2	505-ALNQL(pS)LTHGLSR	745.379 (+2)	b5 (−, 2.2)	b6 (--)	y7 (+1, 4.3)	y8 (+1, 5.4)
pS524 and/or pS525	Low MS2	524-SSRGSIFTFR	619.289 (+2)	b (--)	b4 (−, 1.1)	y (--)	y (--)
pS571	High MS2 Low MS2	569-RP(pS)TQGQPGFGTSAPGHVLNGK	758.365 (+3)	b2 (−, 32.5) b2 (−, 15.5)	b3 (--) b3 (--)	y19 (−, 0.2) y19 (−, 1.8)	y20 (+2, 7.9) y20 (−, 29.2)
pS664	Low MS2	662-AL(pS)AVSVLTSALEELEESHR	741.032 (+3)	b2 (--)	b3 (−, 0.2)	y17 (−, 14.3)	y18 (−, 27.6)
pS664 + pS667	Low MS2	662-AL(pS)AV(pS)VLTSALEELEESHRK	810.384 (+3)	b2 (--)	b4 (−, 0.1) b7 (−, 0.1)	y15 (−, 2.9)	y16 (−, 13.6) y19 (−, 7.7)

[1]The site-discriminating ions observed in the high- and/or low-resolution MS2 spectra of each annotated Nav1.5 phosphopeptide support the assignment of the indicated phosphorylation site(s). The charge state as well as the percentage of maximum intensity of each observed unphosphorylated and phosphorylated site-discriminating (b and y) ion are reported in parenthesis; the (−) symbol indicates that the charge state could not be determined. Abbreviations: Nav, voltage-gated Na^+ channel; LC-MS/MS, Liquid Chromatography-tandem Mass Spectrometry; pS, phosphoserine.